Evaluating GNSS Navigation Availability in 3-D Mapped Urban Environments

Kana Nagai
Mechanical and Aerospace Engineering
Illinois Institute of Technology
Chicago, IL, USA
knagai@hawk.iit.edu

Titilayo Fasoro
Aerospace Engineering
Illinois Institute of Technology
Chicago, IL, USA
tadewalefasoro@hawk.iit.edu

Matthew Spenko
Mechanical and Aerospace Engineering
Illinois Institute of Technology
Chicago, IL, USA
mspenko@iit.edu

Ron Henderson
Landscape Architecture + Urbanism
Illinois Institute of Technology
Chicago, IL, USA
rhender1@iit.edu

Boris Pervan
Mechanical and Aerospace Engineering
Illinois Institute of Technology
Chicago, IL, USA
pervan@iit.edu

***Abstract*—This research project aims to achieve a future urban environment where people and self-driving cars coexist together while guaranteeing safety. To modify the environment, our first approach is to understand the limitations of GPS/GNSS positioning in an urban area where signal blockages and reflections make positioning difficult. For the evaluation process, we assume reasonable integrity requirements and calculate navigation availability along a sample Chicago urban corridor (State Street). We reject all non-line-of-sight (NLOS) that are blocked and reflected using a 3-D map. The availability of GPS-only positioning is determined to be less than 10% at most locations. Using four full GNSS constellations, availability improves significantly but is still lower than 80% at certain points. The results establish the need for integration with other navigation sensors, such as inertial navigation systems (INS) and Lidar, to ensure integrity. The analysis methods introduced will form the basis to determine performance requirements for these additional sensors.**

***Index Terms*—Urban Environments, 3-D Map, multipath, NLOS, DOP**

I. Introduction

The concept of driverless cars draws exciting prospects for the future of urban transportation, but it carries serious doubts as well. These usually arise from questions about safety, especially those related to human lives. Due to the dense environments involved, ensuring navigation safety in urban areas will be much more challenging than in rural areas. The coexistence of people, animals, trees, and buildings together within small areas means crowded spaces. From a GNSS navigation standpoint, these environments also compromise positioning because tall buildings with narrow streets interfere with satellite signals.

One approach to solving the problem is to extract navigation information from the local environment directly. Unfortunately, the arbitrary arrangements of local landmarks do not permit easy quantification of navigation safety. In a dense environment, the probabilities of incorrect landmark extraction and association can be difficult, if not impossible [1], to compute. But what if the environment itself were modified to provide navigation information? For example, by carefully arranging the locations of trees, ranging sensors could be used to determine the vehicle's location with quantifiable integrity, while the trees themselves would provide a greener space for people in the city. Our team, consisting of professionals in the fields of navigation, robotics, and urban design, explores ideal future urban environments where humans and self-driving cars coexist together safely.

For the first step in modifying the environment, we evaluate the GPS/GNSS signal availability in an urban area. This will expose the limitations of GPS/GNSS positioning usage and the places that require the use of sensor fusion such as the combination of GPS, INS (inertial navigation systems) and Lidar. Once these places are identified, the next step will be modifying the environment to increase the probability of correct localization.

Previous research relating to GPS/GNSS signal evaluation in urban environments has been conducted. For example, the concept of "shadow matching" by Groves [2] has been developed to identify GPS signal blockages in urban canyons. The relation between tall buildings and narrow streets complicates GPS positioning. Blockages by tall buildings are not the only reason; building surfaces can also cause positioning degradation due to signal reflections [3]. Three types of GNSS signal receptions are considered in this paper: LOS (i.e., direct signals), non-line-of-sight (NLOS) blocked signals, and NLOS-reflected signals [4]. Fig. 1 illustrates the transmission of the three types of signals.

For the prediction of GPS signal behaviors, 3D environment maps provide the means to trace the path of the invisible multipath rays [5] [6]. 3D maps have been used in previous research to predict GPS availability for real-world signal evaluations [7] [8].

This research is supported by National Science Foundation (Grant No. 1830642).

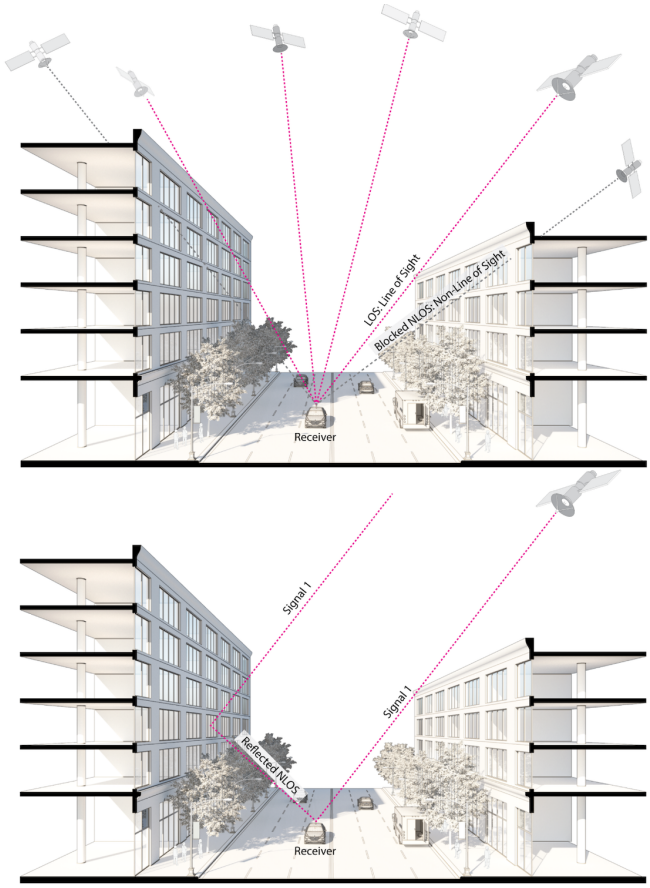

Fig. 1. Three types of GNSS signal reception. The top figure shows direct LOS signals and NLOS-blocked signals. The bottom figure shows NLOS-reflected signals.

In addition to building height and density, signal blockages and reflections are influenced by other factors, including time of a day, the latitude of a city, and the azimuth of a street. These elements have considerable impact on GPS signal availability, especially in urban areas [9]. This study adds to prior work by bringing in the concept of *integrity* in GPS/GNSS signal availability evaluations. Integrity requirements will not necessarily be homogeneous throughout an urban area. There may be different position protection requirements on highways and local streets [10].

The rest of this paper is organized as follows. In section II, the assumptions used in this research are outlined. Sections III and IV discuss direct and reflected signal evaluations, respectively. Finally, section V is the conclusion.

II. Assumptions

We begin by imagining a future driverless car mission scenario; to minimize congestion in the city the autonomous vehicles will be held outside the urban core until requested for action. In the initial open-sky environment, safe navigation can be ensured using real-time kinematic (RTK) GNSS coupled with an INS to provide continuity under overpasses and bridges. Upon entering the urban core, navigation becomes

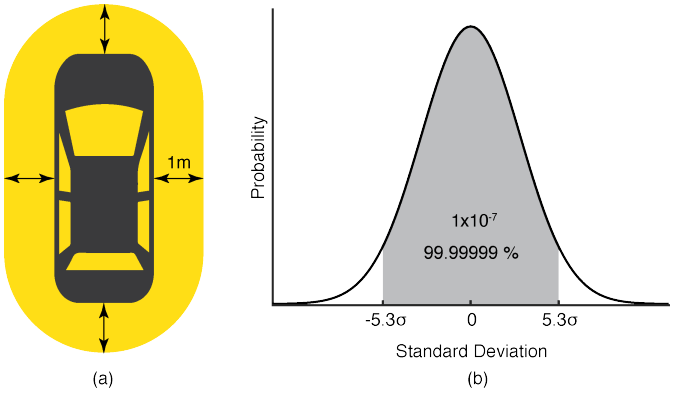

Fig. 2. Integrity requirement assumptions for autonomous vehicle positioning. The position domain alert limit is 1 m in any horizontal direction (a), and the maximum probability of exceedence is 10^{-7} (b).

more dependent on INS performance, vehicle dynamic constraints, and additional sensors for ranging to nearby mapped landmarks—in our case, we intend to use optimally placed trees in the future.

Based on this scenario, there is the initial question of where exactly RTK GPS/GNSS alone can be used for positioning with sufficient integrity. Understanding the answer will help us to establish minimal requirements for additional sensor integration and urban environment modifications.

Navigation performance is traditionally evaluated according to four criteria: accuracy, integrity, continuity, and availability. Accuracy is a measure of a nominal system error, integrity is the ability to know when the system should no longer be used for navigation, and continuity is the ability to function for the duration of the operation. Availability is the fraction of time in which the system is compliant with accuracy, integrity, and continuity requirements before an operation is initiated.

In this work, integrity is studied under scenarios involving either GPS only or GNSS with four constellations (GPS, Galileo, GLONASS, and BeiDou). For the present, we only consider fault-free integrity; satellite faults will be treated in future work. It will become clear shortly that even fault-free integrity is not easy to achieve in urban areas. For quantitative evaluation, we assume as an integrity requirement that the probability of exceeding a 1-meter position estimate error (Fig. 2 (a)) must be lower than 10^{-7} (Fig. 2 (b)). Given a position error standard deviation of σ_{pos}, the 1-meter integrity alert limit corresponds to approximately $5\sigma_{pos}$. Our assumption of a nominal GNSS RTK ranging error standard deviation is approximately $\sigma_\phi = 0.02$ m, and that the differential carrier cycle ambiguities can be readily resolved in the open sky environment before entry into the urban area. The resulting horizontal position dilution of precision (HDOP) required to meet the fault-free integrity requirement is approximately

$$HDOP = \frac{\sigma_{pos}}{\sigma_\phi} < 10. \quad (1)$$

This may seem to be an easily-achievable target for satellite geometry, but it is simply a consequence of the extreme

precision of a GNSS carrier phase. Nevertheless, once the vehicle enters the urban environment, the effects of LOS blockages and reflected signals can make it quite difficult to achieve DOP less than 10 in practice. At a minimum, it is necessary to quantify the availability of both GPS and GNSS satellite geometries that meet the DOP constraint in a real urban environment.

III. Direct Signal Evaluation

A. LOS and NLOS Signal Separation

The work begins by applying shadow matching techniques [2] for identification and separation of LOS and NLOS-blocked signals. Since GNSS satellites are distant enough from the receiver, their received signals are analogous to sunlight rays, and the areas obstructed by buildings are similar to shadows. We first examine the shadows using a 3D map of Chicago's downtown [11] with computer-aided design (CAD) software at a moment when a total of six GPS satellites are potentially visible.

In Fig. 3 (b), the colors represent the number of visible satellites ranging from 1 to 6, which are red to blue, respectively. The street that runs from north to south consists of tall buildings on its north end and residential areas with buildings less than 3 stories on the south end [13] (see Fig. 3 (a)). The number of building stories affects the transitions between open sky and urban canyon areas along the street. The figure is helpful to get a general idea of satellite visibility in this part of the city, but we now move on to examining integrity at specific points in the area.

B. Integrity Calculation

To quantify fault-free integrity using DOP, we need satellite geometry information at a receiver location of interest. Then LOS and NLOS signals must be separated. Using a 3D map and overshadowing tools [14], we project the field of view from one particular point of interest, for instance, the vehicle's antenna, onto a hemisphere representing the sky. This projection shows building occupancy on a sky plot, and when overlapped with a sky plot of satellite LOS locations from GNSS almanac data, it illustrates satellite visibility at a given time (Fig. 4).

If a building blocks a satellite, the satellite exists within the building's domain; these satellites are not included in subsequent positioning calculations. Only LOS signals remain, and these are used to calculate DOP using the following equation:

$$\mathbf{H} = (\mathbf{G}^T\mathbf{G})^{-1} \tag{2}$$

where $\mathbf{G}$ is the LOS geometry matrix. The diagonal elements of matrix $\mathbf{H}$ can be expressed as:

$$\mathbf{H} = \begin{bmatrix} \mathrm{NDOP}^2 & \bullet & \bullet & \bullet \\ \bullet & \mathrm{EDOP}^2 & \bullet & \bullet \\ \bullet & \bullet & \mathrm{VDOP}^2 & \bullet \\ \bullet & \bullet & \bullet & \mathrm{TDOP}^2 \end{bmatrix} \tag{3}$$

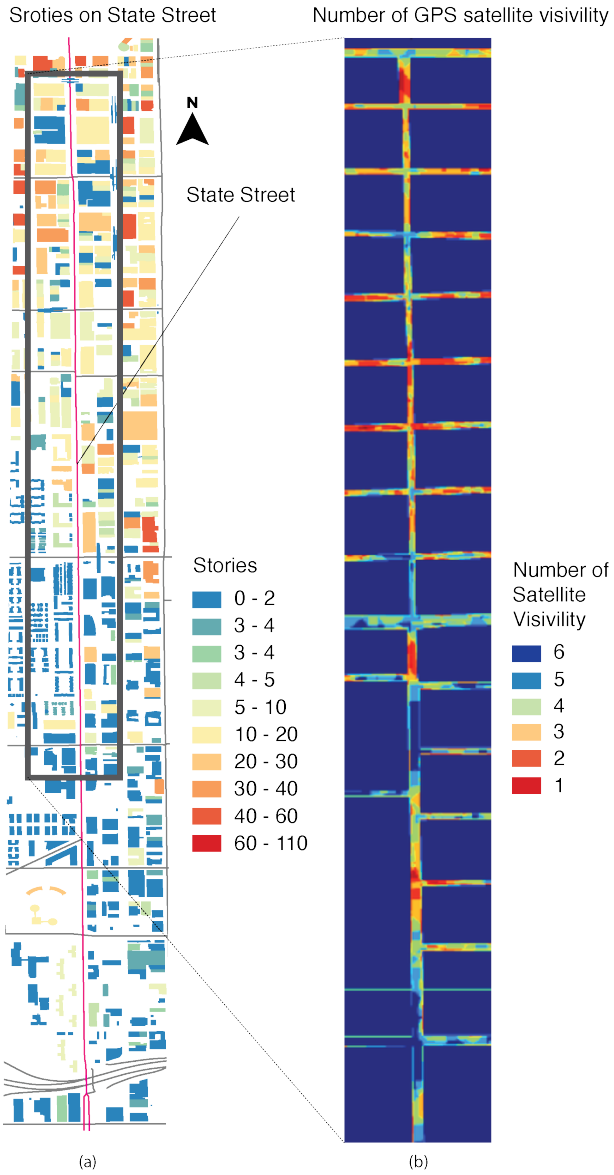

Fig. 3. Building footprints and stories on the State Street (a). GPS satellite visibility using ephemeris data on January 2, 2019 at midnight (b) [12].

where NDOP, EDOP, VDOP and TDOP are East, North, Vertical, and Time DOP respectively. Since the vehicle is restricted to motion on the ground, we are only interested in EDOP, NDOP, and (horizontal) HDOP, which is defined as:

$$\mathrm{HDOP} = \sqrt{\mathrm{NDOP}^2 + \mathrm{EDOP}^2}. \tag{4}$$

HDOP, EDOP, and NDOP are affected by the direction of the street [2]. We calculate the DOPs every 2 minutes over 24 hours and determine the fraction of time at each point that DOP is less than 10. When the total availability is more than or equal to 97%, it guarantees 1400 out of 1440 minutes of GNSS signal availability over 24 hours. A flow chart illustrating the process is shown in Fig. 5.

The selected simulation area is a 170 m north-south sub-

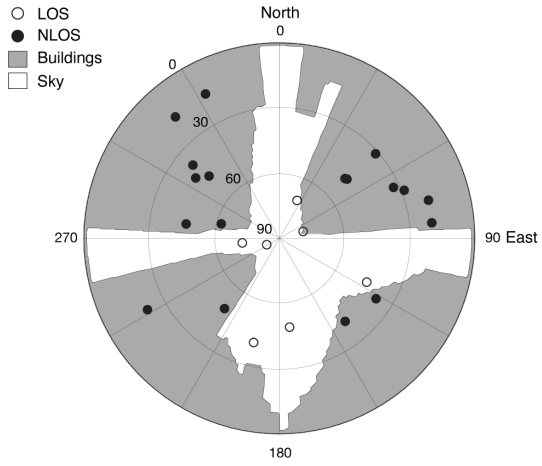

Fig. 4. An example of a sky plot overlapped with building domains and GNSS satellite positions using four constellations. Black dots are NLOS-blocked satellites, and clear circles are LOS satellites. The gray areas are building domains. NLOS-blocked satellites are excluded from the DOP calculations.

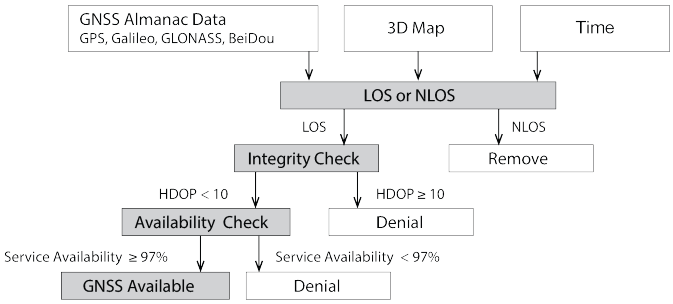

Fig. 5. Flow chart of GNSS availability calculation. There are three processes: LOS/NLOS separation, integrity check, and availability calculation.

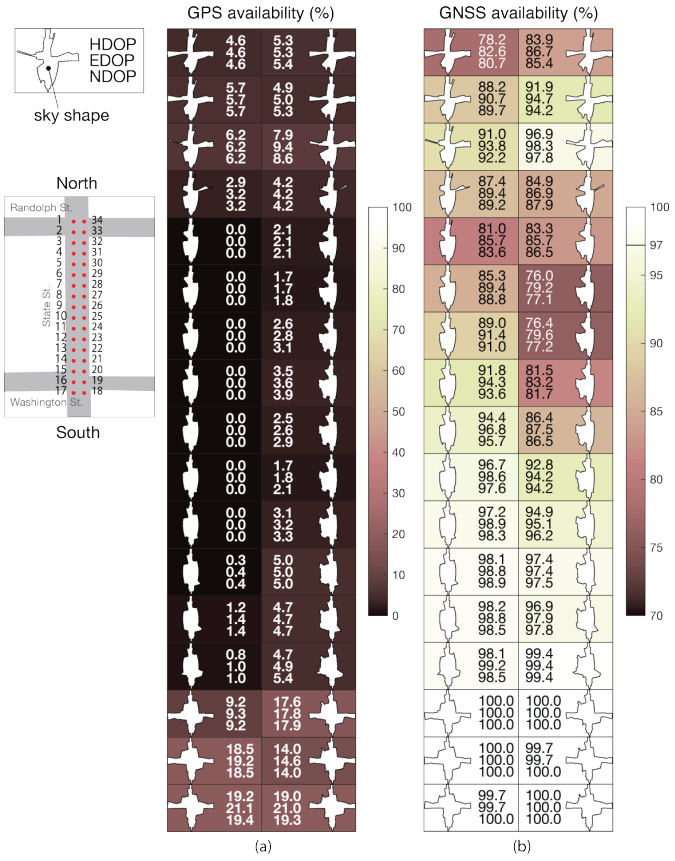

Fig. 6. Percentage of time navigation function is available with integrity using GPS only (a) and four GNSS constellations (b). Availability was computed at 34 receiver points on State Street between two intersections. The outermost columns show the open sky shapes. The inner columns list HDOP, EDOP, and NDOP availability (top to bottom) at each evaluation point.

section of the State Street transect. This section of the street contains buildings of different heights, averaging about 36 m height on the east and 14 m on the west. The evaluation considers a total of 34 points placed at 10 m intervals in two lanes.

C. Availability Results

The results show poor availability when using GPS only, ranging from 0% to 5% along the block and 5% to 20% at the intersections (Fig. 6 (a)). The points with 0% do not acquire more than or equal to four LOS of satellites, the minimum requirement for GPS positioning at any time during the day. Clearly the number of satellites using GPS alone is not nearly enough for navigation in this environment.

We next evaluate the future potential availability using four full GNSS constellations: GPS, Galileo, GLONASS, and BeiDou. In this case, the availability of each DOP < 10 is significantly better, ranging from 21% to 92% along the block and 48% to 99% at the intersections. However, it is still insufficient to support continuous autonomous driving. (Fig. 6 (b)).

Signal availability at the intersections is repeatedly revealed to be better than other parts of the street since more sky area is present. Satellite visibility is usually expected to be better along the direction of the street than across, but the results show that there is actually no significant difference between EDOP and NDOP values. We will discuss the factors that influence signal availability in the next section.

D. Availability Analysis

According to Groves [2], the direction in which a street lies causes a higher dilution of precision in the direction of that street. For example, a street running east-westward will generally have a larger EDOP than NDOP. This conjecture proved to be generally accurate in separate simulations we performed on Madison Street which lies along the east-west direction, but State Street (north-south) does not show a noticeably larger NDOP than EDOP. For this reason, we further explored street direction and other factors that may affect the DOP along State Street. This section outlines and discusses the factors that affect availability in urban areas. Building height is one of them as demonstrated earlier (see Fig. 3), but additional factors exist [9].

As satellites move in their orbits, their entire configuration in the sky changes over time. A static observer would obviously see different satellite geometries at different times.

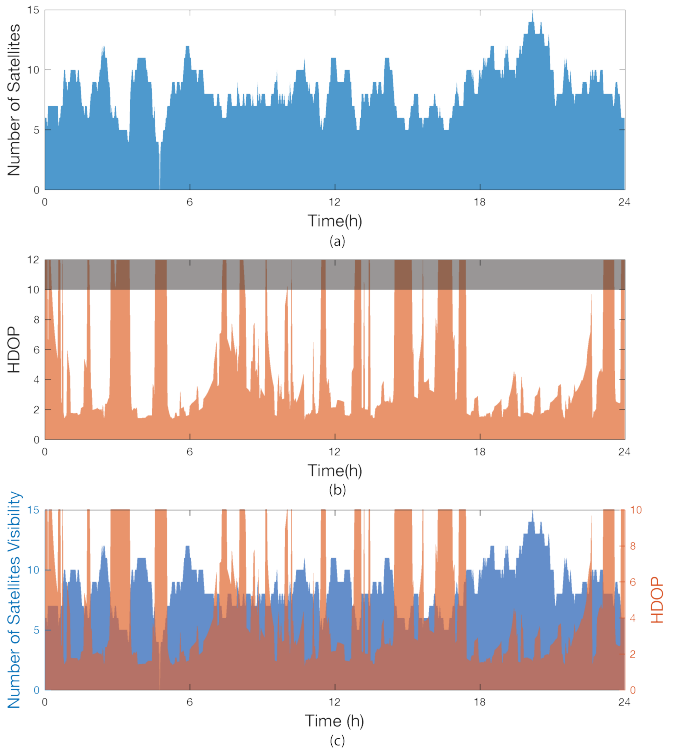

Fig. 7. GNSS satellite visibility changing over time (a), and HDOP also changing over time (b). The bottom figure overlaps the two figures illustrating the correspondence between the number of satellite visible and HDOP (c).

Fig. 7 shows the number of visible GNSS satellites and HDOP for a static receiver on State Street over a 24 hr time period. Around the 20 hour mark, the maximum number of satellites is experienced, and the minimum number of satellites is achieved around the 5 hour mark. When the HDOP and satellite visibility plots are overlapped, a lower number of visible satellites generally corresponds to a larger HDOP.

Latitude dependency can be demonstrated by using the same layout location, time, and longitude, while changing the latitude. Fig. 8 compares the DOP featuring the same street at 0, 41.87 (Chicago), and 60-degree latitude locations. The results generally show a better DOP at lower latitudes than higher ones. This significant difference is due to the inclinations of the satellite orbits. When viewed from the ECEF frame, the orbits of the satellite constellations leave voids in the northern and southern polar areas.

As noted above, the direction (azimuth) of the street is also a factor associated with availability. In Fig. 9, State Street is rotated from north to south at 0, 30, and 90-degree angles. The results clearly show the effect of street direction, with the 0-degree rotation having the worst availability amongst the three.

In summary, while building height is prime factor affecting satellite availability, other factors including time of day, latitude, and the azimuth angle of a street, also have a significant impact.

Additionally, although we have adopted the simple criterion

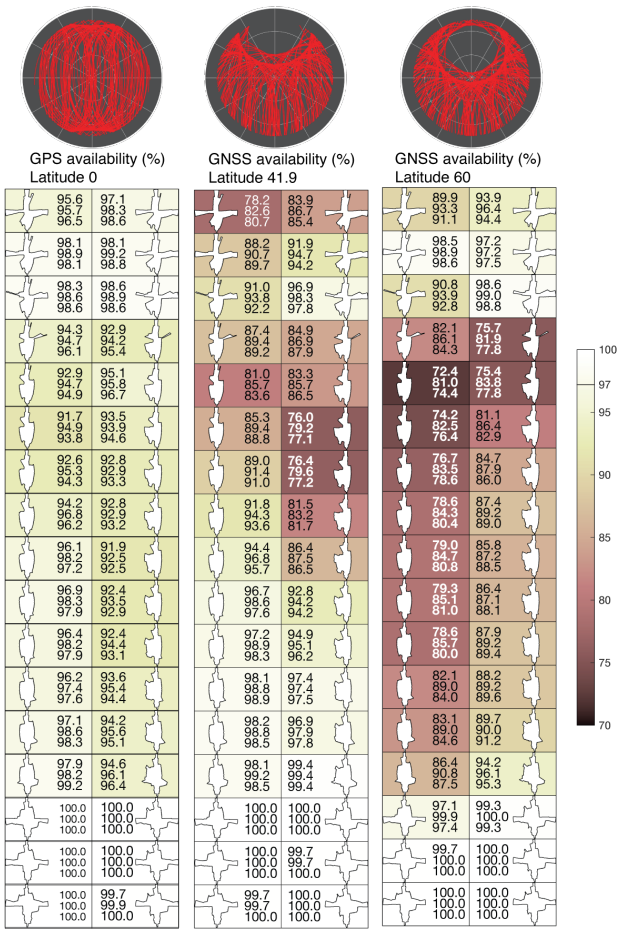

Fig. 8. GNSS availability over different latitudes.

DOP $<$ 10 to determine whether a satellite configuration is available for navigation with integrity, if the DOP threshold is tightened or loosened, or if different or additional criteria are added, availability would also be affected.

Furthermore, so far we have only dealt with LOS and NLOS-blocked signals, ignoring that some of the signals deemed LOS may also produce dangerous multipath reflections from nearby buildings. In the next section, we describe a way of excluding NLOS-reflected signals in a urban environments.

IV. Reflected Signal Evaluation

A. *Specular Reflection Detection*

To ensure positioning integrity, NLOS signals reaching a vehicle's receiver via specular reflection must be excluded from DOP and positioning calculations . Specular reflections are not the only signal reflection that can affect integrity, but these are the only types of reflections we consider for now. The impact of diffuse reflections will need eventually be evaluated as well.

First, we predict the reflected LOS vector of GNSS signals using the Householder transformation [15]. When the incident ray vector and the reflection plane are known, the Householder

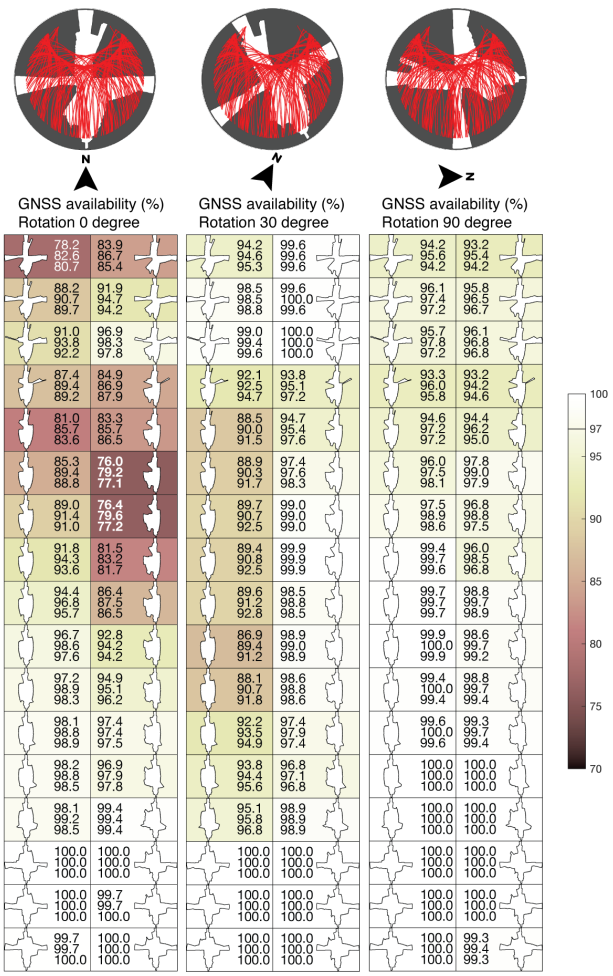

Fig. 9. GNSS availability comparison for different street azimuths.

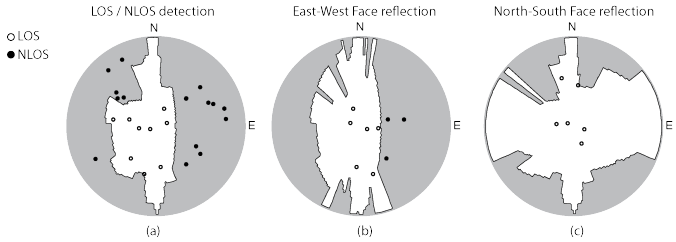

Fig. 10. This sequence of sky plots explains how to predict the existence of NLOS-reflected signals. Gray areas represent building or building wall occupation from a receiver point, and if the reflection vector penetrates the walls, it is an NLOS-reflected signal.

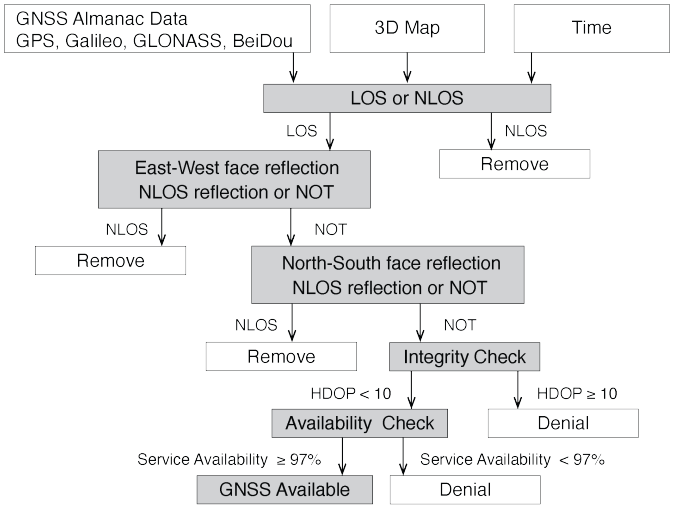

Fig. 11. Flow chart showing availability calculation considering the reflected signal effect. Potential reflections from both east-west facing and north-south facing walls are accounted for.

transformation returns the specular reflection vector using the equation:

$$\|\mathbf{a}\|\,\mathbf{v} = (\mathbf{I} - 2\mathbf{u}\mathbf{u}^T)\mathbf{a} \tag{5}$$

where $\mathbf{v}$ is the vector direction of the reflected ray, $\mathbf{u}$ is a vector direction normal to the reflection plane, and $\mathbf{a}$ is a vector along the direction of the incident ray. The user and satellite locations determine the incident ray vector, and the 3D environment map provides the vector of the normal direction plane from which the ray can potentially reflect. Consequently, all inputs are known, and the reflected signal direction is determined (Fig. 10 (b)).

We then use building occupancy sky plots to check whether the hypothesized reflection ray vector actually strikes a physical wall or not (Fig. 10 (b) and (c)). If the ray penetrates a mapped wall, then the antenna receives the NLOS-reflected ray from a phantom satellite direction. Therefore, the receiver must declare this satellite unusable to ensure positioning integrity. After the removal of all blocked and reflected NLOS satellites, we can again evaluate DOP or any other positioning performance metric (Fig. 11).

B. Specular Reflection Availability Results and Analysis

Fig. 12 shows the results of GNSS signal availability when we exclude satellites that produce reflected NLOS signals; the computed availability drops at every point. The heat map in Fig. 12 visually illustrates the decrements, which are not homogeneous: some points decrease only a few percent and others more than 50%. These decreases are concentrated on the east side of the street along the block. This asymmetry suggests that there must be an environmental factor leading to it. Indeed, the street is located between buildings of different heights, averaging about 36 m height on the east and 14 m on the west (Fig. 13). The height difference between two buildings facing each other induces NLOS reflections, and the receiver located on the side of the street closer to the taller building tends to see a more significant decrease in GNSS availability. If the shorter building does not disturb a LOS signal the taller building's face can reflect the ray back. As a result, both the LOS and reflected NLOS signals will reach the antenna, and so to ensure integrity we must reject the satellite from use. This is why availability decreases.

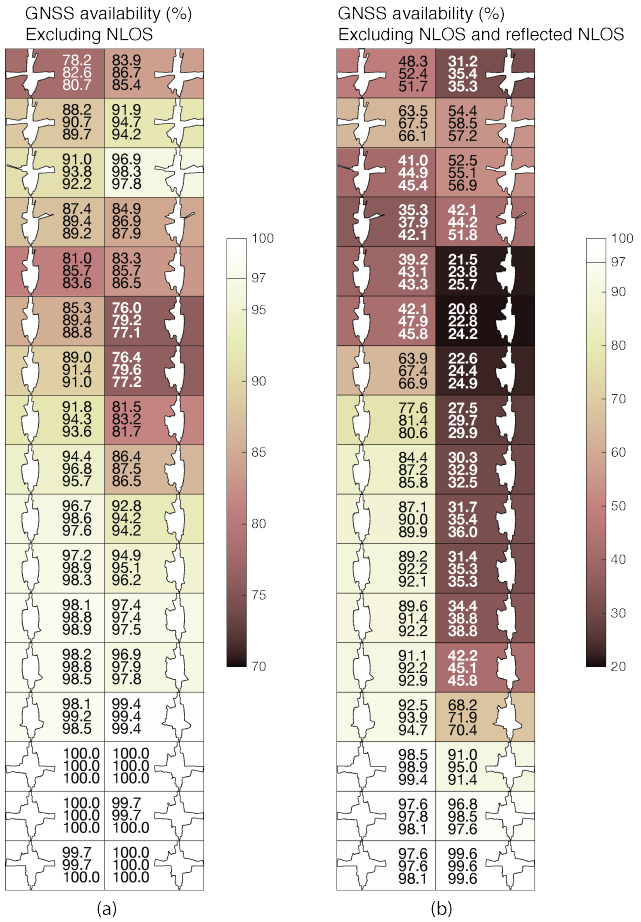

Fig. 12. Percentage of signal availability in 24 hours excluding NLOS-blocked (a) and excluding NLOS-blocked and NLOS-reflected satellites (b).

C. Future Work

The need to reject satellites with NLOS-reflected signals (to maintain integrity) decreases GNSS availability in specific areas, and travelling between tall buildings with differential across-street heights generates navigation discontinuities. It is also noteworthy that State Street is wider than other streets in downtown Chicago, and the buildings along it are not particularly tall relative to those along many other nearby streets.

One countermeasure for continuity preservation is sensor fusion. If GNSS positioning is integrated with INS to bridge DOP gaps, continuity can be considerably improved. In the next phase of our work, we plan to implement a tightly coupled GNSS-INS mechanization using an Extended Kalman filter [16]. We aim to evaluate the extent to which a GNSS system augmented with dead reckoning can navigate safely and continuously through a real urban environment. Regions of excessive inertial drift will be determined and will need to be mitigated with local Lidar ranging.

V. Conclusion

This research evaluates the availability of fault-free integrity of GPS/GNSS positioning along a representative urban street

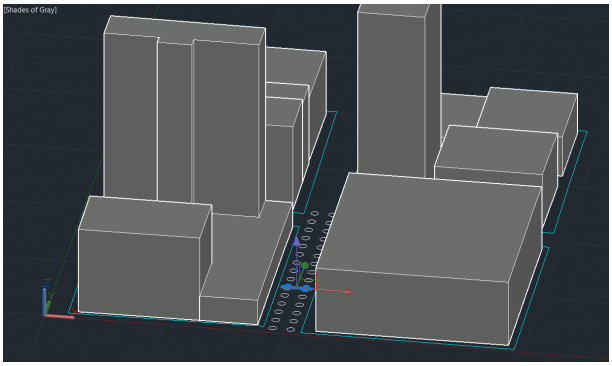

Fig. 13. Reflected NLOS signals occur most often when there is significant disparity in height between buildings across the street from each other.

(State Street in Chicago) to determine where and under what conditions the sensor can provide safe navigation. Some GNSS signals are blocked and others are reflected in challenging urban environments. Blocked signals are easily predicable using 3D maps. To predict reflected signals, we use the combination of 3D maps and Householder transformations. Taking into account satellite blockages only, the availability of GPS positioning is less than 10%, and for GNSS positioning with four full constellations, it varies between 75% and 100% at various locations along the street. When satellites contributing reflected signals are also excluded, the GNSS availability is reduced to between 20% and 97%. Although GNSS provides much better positioning availability than GPS-only, it cannot provide continuous vehicle positioning along the street. Augmentation with INS and other sensors, including local Lidar ranging, will be investigated next to improve availability.

Acknowledgment

Fig. 1 was created by Alexis Arias, Landscape Architecture + Urbanism, Illinois Institute of Technology. The authors are grateful to Professor Nilay Mistry, Landscape Architecture + Urbanism, Illinois Institute of Technology, for his helpful advice on this research.

This research project is funded by the National Science Foundation (Grant No. 1830642).

References

[1] G. Duenas Arana, O. A. Hafez, M. Joerger, and M. Spenko, "Recursive Integrity Monitoring for Mobile Robot Localization Safety," 2019 International Conference on Robotics and Automation (ICRA) 10.1109/ICRA.2019.8794115

[2] P. D. Groves, "Shadow Matching: A New GNSS Positioning Technique for Urban Canyons," Journal of Navigation, vol. 64, no. 3, pp. 417–430, Jul. 2011.

[3] R. Ercek, P. D. Doncker, and F. Grenez, "NLOS-multipath effects on Pseudo-Range estimation in urban canyons for GNSS applications," European Space Agency, (Special Publication) ESA SP, vol. 626 SP, no. Novem-ber, pp. 1–6, 2006.

[4] S. Ollander, F.-W. Bode, and M. Baum, "Multi-Frequency GNSS Signal Fusion for Minimization of Multipath and Non-Line-of-Sight Errors: A Survey," 2018 15th Workshop on Positioning, Navigation and Communications (WPNC), 2018.

[5] S. Bauer, M. Obst, and G. Wanielik, "3D environment modeling for GPS multipath detection in urban areas," International Multi-Conference on Systems, Sygnals and Devices, 2012.
[6] S. Miura, S. Hisaka, and S. Kamijo, "GPS multipath detection and rectification using 3D maps," 16th International IEEE Conference on Intelligent Transportation Systems (ITSC 2013), 2013.
[7] I. Smolyakov, M. Rezaee, and R. B. Langley, "Resilient Multipath Prediction and Detection Architecture for Low-cost Navigation in Challenging Urban Areas," Proceedings of the 32nd International Technical Meeting of the Satellite Division of The Institute of Navigation (ION GNSS 2019), pp. 175–188, 2019.
[8] G. Zhang, "3D Mapping Aided GNSS-Based Cooperative Positioning Using Factor Graph Optimization," Proceedings of the 32nd International Technical Meeting of the Satellite Division of The Institute of Navigation (ION GNSS 2019), pp. 2269–2284, 2019.
[9] J. Jakobsen, A. B. O. Jensen, and A. A. Nielsen, "Simulation of GNSS reflected signals and estimation of position accuracy in GNSS-challenged environment," Journal of Geodetic Science, vol. 5, no. 1, pp. 47–56, 2015.
[10] T. G. Reid, S. E. Houts, R. Cammarata, G. Mills, S. Agarwal, A. Vora, and G. Pandey, "Localization Requirements for Autonomous Vehicles," SAE International Journal of Connected and Automated Vehicles, vol. 2, no. 3, 2019.
[11] "Worldwide map files for any design program," cadmapper. [Online]. Available: https://cadmapper.com/. [Accessed: 30-Dec-2019].
[12] International GNSS service "Data Repository". [Online]. Available: https://cddis.nasa.gov. [Accessed: 30-Dec-2019].
[13] "Building Footprints (current): City of Chicago: Data Portal," Chicago. [Online]. Available: https://data.cityofchicago.org/Buildings/Building-Footprints-current-/hz9b-7nh8. [Accessed: 30-Dec-2019].
[14] "Dynamic Overshadowing," andrewmarsh.com. [Online]. Available: http://andrewmarsh.com/software/shading-box-web/. [Accessed: 08-Jan-2020].
[15] A.S.Householder, "Unitary Triangularization of a Nonsymmetric Matrix," Journal of the ACM, vol. 5, no. 4, pp. 339–342, Jan. 1958.
[16] Tanil, Cagatay, et al. "Optimal INS/GNSS Coupling for Autonomous Car Positioning Integrity." Proceedings of the 32nd International Technical Meeting of the Satellite Division of The Institute of Navigation (ION GNSS+ 2019), pp. 3123–3140, 2019.